nature neuroscience

TECHNICAL REPORT

From synapse to behavior: rapid modulation of defined neuronal types with engineered $GABA_A$ receptors

Peer Wulff[1,6,7], Thomas Goetz[1,6,7], Elli Leppä[2], Anni-Maija Linden[2], Massimiliano Renzi[3], Jerome D Swinny[4], Olga Y Vekovischeva[2], Werner Sieghart[5], Peter Somogyi[4], Esa R Korpi[2], Mark Farrant[3] & William Wisden[1,6]

In mammals, identifying the contribution of specific neurons or networks to behavior is a key challenge. Here we describe an approach that facilitates this process by enabling the rapid modulation of synaptic inhibition in defined cell populations. Binding of zolpidem, a systemically active allosteric modulator that enhances the function of the $GABA_A$ receptor, requires a phenylalanine residue (Phe77) in the γ2 subunit. Mice in which this residue is changed to isoleucine are insensitive to zolpidem. By Cre recombinase–induced swapping of the γ2 subunit (that is, exchanging Ile77 for Phe77), zolpidem sensitivity can be restored to $GABA_A$ receptors in chosen cell types. We demonstrate the power of this method in the cerebellum, where zolpidem rapidly induces significant motor deficits when Purkinje cells are made uniquely sensitive to its action. This combined molecular and pharmacological technique has demonstrable advantages over targeted cell ablation and will be invaluable for investigating many neuronal circuits.

A classical approach to the study of brain function is selective lesioning. Unfortunately, the interpretation of data from such studies can be confounded by compensatory changes, whereby unrelated systems are recruited to alleviate, if only partially, any deficit. A complementary method involves reversibly silencing, albeit with little or no cell-type selectivity, the activity of a pathway or nucleus through cooling or stereotaxic drug administration (for example, see refs. 1,2). Reversible approaches have advantages over permanent lesioning. First, the effects of acute regional inactivation cannot be easily overcome by compensatory changes, because the inactivated system is altered only briefly (reviewed in refs. 3,4). Second, we can learn, in principle, not only 'where', but also 'when' and for 'how long' a brain region is involved in a given function[3]. Similar considerations apply to the functional dissection of brain circuit components. Thus, to determine how specific cell types influence network properties and contribute to animal behavior, a method is needed for reversibly inactivating a single neuronal type in a specific brain area[5]. This approach poses two challenges: first, there are many cells of each type; and second, neuronal classes are often dispersed as sparse populations in large volumes (such as subtypes of GABAergic interneurons in the hippocampus).

The effects on brain function of drugs acting on $GABA_A$ receptors show that it is not necessary to silence a cell type to alter network properties or behavior: a modest modulation of inhibitory postsynaptic currents (IPSCs) is sufficient[6–8]. $GABA_A$ receptors, which are present on all neurons in the mammalian brain, are ligand-gated anion-permeable channels and produce fast inhibition. They are commonly formed from two α, two β and a single γ2 subunit (encoded by *Gabrg2*)[6–8]. The α1βγ2, α2βγ2 and α3βγ2 subunit combinations account for most $GABA_A$ receptors; of these, the main subtype is α1β2γ2 (refs. 6–8). Benzodiazepines, benzodiazepine-site ligands (such as the imidazopyridine zolpidem) and anesthetics are positive allosteric modulators of $GABA_A$ receptors[6–10]. These drugs cause a conformational alteration in the $GABA_A$ receptor such that GABA-induced anion flux is enhanced[11]. Elegant studies of 'knock-in' mice, carrying amino acid changes at drug-binding sites in the α or β subunits, show how subtype-specific modulation of $GABA_A$ receptors differentially influences mouse behavior[6,12–15]. These studies are 'subtractive': by changing genes encoding α or β subunits across the whole brain and observing the diminished effect of benzodiazepines, zolpidem or anesthetics on the mouse, the contributions of $GABA_A$ receptor subtypes to specific behaviors (related to anxiety, sedation, anesthetic actions or motor control) can be deduced[6,12–15].

To develop a method for functional dissection of circuit components, we considered reversing this $GABA_A$ receptor knock-in strategy by generating zolpidem-insensitive mice and then genetically imposing zolpidem sensitivity on a selected cell type. We chose zolpidem as the ligand because of the way in which it binds to the $GABA_A$ receptor. One $GABA_A$ receptor subunit, the γ2 subunit, is expressed almost universally in brain[16,17] and is incorporated into most $GABA_A$ receptors. Zolpidem binding occurs throughout the brain[17,18] inside a pocket created between an α subunit (α1, α2 or α3) and the

[1]Department of Clinical Neurobiology, University of Heidelberg, Im Neuenheimer Feld 364, 69120 Heidelberg, Germany. [2]Institute of Biomedicine, Pharmacology, Biomedicum Helsinki, POB 63 (Haartmaninkatu 8), University of Helsinki, FI-00014 Helsinki, Finland. [3]Department of Pharmacology, University College London, Gower Street, London WC1E 6BT, UK. [4]MRC Anatomical Neuropharmacology Unit, Oxford University, Mansfield Road, Oxford OX1 3TH, UK. [5]Center for Brain Research, Section of Biochemistry and Molecular Biology of the Nervous System, Medical University of Vienna, Spitalgasse 4, A-1090 Vienna, Austria. [6]Present address: Institute of Medical Sciences, University of Aberdeen, Foresterhill, Aberdeen AB25 2ZD, UK. [7]These authors contributed equally to this work. Correspondence should be addressed to P.W. (p.wulff@abdn.ac.uk).

Received 8 February; accepted 22 May; published online 17 June 2007; doi:10.1038/nn1927

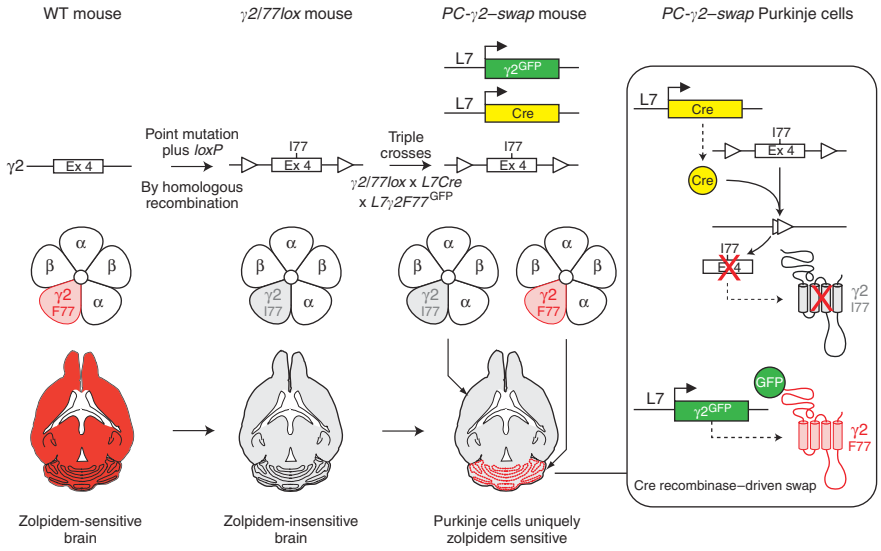

Figure 1 Strategy to restrict zolpidem sensitivity to selected neural types, using Cre recombinase to drive a γ2I77 to γ2F77 subunit swap. The genotype, the pentameric $GABA_A$ receptors formed from α, β and γ2 (γ2F77 or γ2I77) subunits and corresponding brain sections, with zolpidem sensitivity indicated in red, are shown for three groups of mice. Homologous recombination in embryonic stem cells is used to introduce a Phe77 to isoleucine point mutation and to flank exon 4 with *lox*P sites. The resultant mice are crossed with mice expressing Cre recombinase and the zolpidem-sensitive γ2 subunit under the control of the Purkinje cell–selective L7 promoter to generate *PC-γ2–swap* mice. In the Purkinje cells of these mice, Cre catalyzes recombination between the *lox*P sites, resulting in excision and loss of exon 4, and thus deletion of the γ2I77 subunit (gray). In its place, the $\gamma 2F77^{GFP}$ transgene produces the wild-type zolpidem-sensitive γ2 subunit (red), tagged with GFP at its amino terminus.

γ2 subunit[19]. The γ2 subunit contributes an essential residue (Phe77) to this pocket[20,21]. As shown with cloned $GABA_A$ receptors, if Phe77 of γ2 is mutated to isoleucine, the receptors function normally with respect to activation by GABA but they are no longer modulated by zolpidem[20,21]. Pharmacological, electrophysiological and behavioral tests have shown that mice with an engineered γ2 Ile77 mutation are insensitive to zolpidem[22–24]. The Ile77 mutation does not affect the action of GABA at $GABA_A$ receptors: in γ2 Ile77 mice, miniature IPSCs (mIPSCs) have normal rise times, amplitudes and decay kinetics[22,23].

We therefore considered that, by cell type selectively replacing ('swapping') the Ile77 γ2 subunit in zolpidem-insensitive mice with the zolpidem-sensitive (Phe77) variant, we would be able to use zolpidem to modulate reversibly the activity of any defined neuronal population. To test the feasibility of this method, we chose to use Purkinje cells, which offer straightforward genetic targeting[25] and a quantifiable behavioral readout—namely, motor performance on the rotarod. Purkinje cells provide the only output of the cerebellar cortex. Dendritic and perisomatic synaptic inhibition, provided by stellate and basket cells, respectively, alters the intrinsic activity of Purkinje cells[26] and shapes their response to excitatory synaptic input[27,28]. Purkinje cells express α1β2γ2- and α1β3γ2-type $GABA_A$ receptors[29,30] that underlie fast GABAergic IPSCs.

Here we describe how we have made $GABA_A$ receptors on Purkinje cells uniquely sensitive to zolpidem and then have used this drug to produce rapid and reversible behavioral effects through selective modulation of inhibitory synaptic input. To emphasize the advantages of this approach, we have also generated a static (long-term) knockout of fast GABAergic input onto Purkinje cells by producing cell type–selective deletion of their γ2 subunits, and have compared the effects of the two manipulations on the same behavioral tests under identical conditions.

RESULTS

Explanation of the strategy applied to Purkinje cells

The strategy was to produce mice devoid of zolpidem-sensitive $GABA_A$ receptors by engineering the γ2 subunit gene (*Gabrg2*) such that the codon for Phe77 encoded isoleucine. The gene was also engineered to contain *lox*P sites, allowing its inactivation by Cre recombinase (**Fig. 1**). Coexpression of the zolpidem-sensitive γ2 Phe77 (hereafter γ2F77) subunit and Cre recombinase in Purkinje cells should thus lead to a subunit swap, such that Cre-positive, γ2F77-positive Purkinje neurons would not contain γ2 Ile77 (hereafter γ2I77) subunits, which would have been deleted by Cre recombinase (**Fig. 1**). We termed these Purkinje γ2 swap mice '*PC-γ2–swap*' mice: only their Purkinje cells should express zolpidem-sensitive $GABA_A$ receptors.

Deletion of the $GABA_A$ receptor γ2 subunit in Purkinje cells

The *γ2I77lox* line served as both a *loxP*-flanked (floxed) allele for cell type–specific ablations of $GABA_A$ receptor γ2 subunits (*γ2I77lox* × cell type–specific promoter driving Cre) and the foundation line for producing cell type–selective zolpidem sensitivity (*γ2I77lox* × cell type–specific promoter driving Cre × cell type–specific promoter driving γ2F77 subunit 'swapping'; see **Fig. 2**, and **Supplementary Methods** and **Supplementary Fig. 1** online).

The γ2 subunit targets $GABA_A$ receptors to postsynaptic sites and confers full (25–30 pS) single-channel conductance on the receptor[31,32]. To compare and to contrast the dynamic modulation of GABAergic input onto Purkinje cells with the long-term removal of such input, we also generated mice with a Purkinje-cell–specific deletion of γ2, and thus a deletion of synaptic $GABA_A$ receptors. Mice with Cre recombinase expressed selectively in Purkinje cells (*L7Cre* mice[33]; see **Supplementary Fig. 2** online) were crossed with *γ2I77lox* mice, producing a Purkinje cell–selective 'static' knockout of synaptic responsiveness to GABA (these mice were termed '*PC-Δγ2*' mice; **Fig. 2**).

Purkinje cell–restricted $\gamma 2F77^{GFP}$ expression

For the zolpidem-sensitive γ2F77 subunit swap, we tagged the γ2F77 subunit at its amino terminus with enhanced green fluorescent protein, eGFP ($\gamma 2F77^{GFP}$; see **Supplementary Methods** and ref. 34) to distinguish it from the endogenous γ2I77 subunit. By using the L7 Purkinje cell–specific promoter[25], mice were produced with expression of $\gamma 2F77^{GFP}$ restricted to Purkinje cells. One of the $L7\gamma 2F77^{GFP}$ lines (of six screened) gave strong expression of the mRNA specifically in Purkinje cells, as detected by *in situ* hybridization with a *GFP*-specific probe. We then made triple crosses ($\gamma 2I77lox \times L7Cre \times L7\gamma 2F77^{GFP}$ (see Methods)) to generate *PC-γ2–swap* mice (**Fig. 2**). At the cellular level, we first established that the $\gamma 2F77^{GFP}$ subunit in these mice was targeted to GABAergic synapses, and that IPSCs onto Purkinje cells were uniquely sensitive to zolpidem.

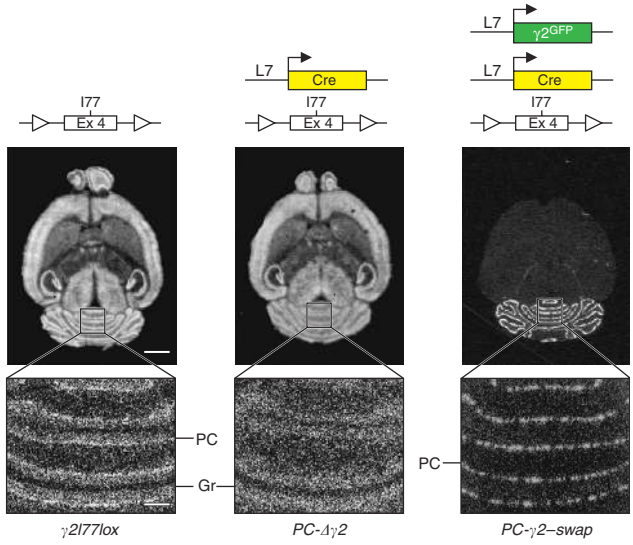

Figure 2 Summary of mouse genotypes. *In situ* hybridization autoradiographs show the expression of various $GABA_A$ receptor γ2 subunit mRNA in brain sections from *γ2I77lox*, *PC-Δγ2* and *PC-γ2–swap* adult mice. The corresponding transgene content (genotype) of the mice is indicated above the images (arrowheads, *lox*P sites; Ex 4, exon 4). The *γ2I77lox* and *PC-Δγ2* autoradiographs were obtained with a γ2-specific (exon 4) oligonucleotide. To visualize selectively the $\gamma2F77^{GFP}$ mRNA, the *PC-γ2–swap* image was obtained with a GFP-specific oligonucleotide. Magnifications of the boxed areas are shown at the bottom. In *γ2I77lox* cerebellum, exon 4–containing *γ2I77* mRNA is present in all layers of the cerebellum, but is most evident in the granule cell (Gr) and Purkinje cell (PC) layers. In *PC-Δγ2* cerebellum, *γ2I77* mRNA is absent from the Purkinje cell layer. In *PC-γ2–swap* brains, $\gamma2F77^{GFP}$ mRNA is present only in Purkinje cells. Scale bars, 2 mm and 300 μm.

$\gamma2F77^{GFP}$ is enriched at GABAergic synapses

Primary GFP fluorescence and GFP immunoreactivity in *PC-γ2–swap* mice was selectively localized to Purkinje cells throughout the cerebellum (**Supplementary Fig. 3** online). The rest of the brain in *PC-γ2–swap* mice (or littermate control mice) had no GFP immunoreactivity. Purkinje cells of *PC-γ2–swap* mice contained granular GFP immunoreactivity in both their cell body (excluding the nucleus) and their proximal dendrites, presumably corresponding to $\gamma2F77^{GFP}$ associated with endo-membranes (**Fig. 3**). Strongly immunopositive puncta and 0.5–1-μm segments of membrane were present in the soma and the main dendrites (**Fig. 3**). Scattered GFP-positive puncta were also present throughout the molecular layer and presumably corresponded to smaller dendrites of Purkinje cells (**Fig. 3**).

To confirm that the $\gamma2F77^{GFP}$ subunits were located in GABAergic synapses, we performed triple immunolabeling (**Fig. 3**). The GFP-positive segments always colocalized with the endogenous α1 subunit of the $GABA_A$ receptor. Immunoreactivity for the α1 subunit was also present as short segments and puncta in the molecular layer outside the GFP patches, corresponding to GABAergic synapses on other cerebellar neurons. Most GFP patches, both on Purkinje cells and in the neuropil, were apposed to glutamic acid decarboxylase (GAD)-immunoreactive structures, representing GABAergic nerve terminals (**Fig. 3**).

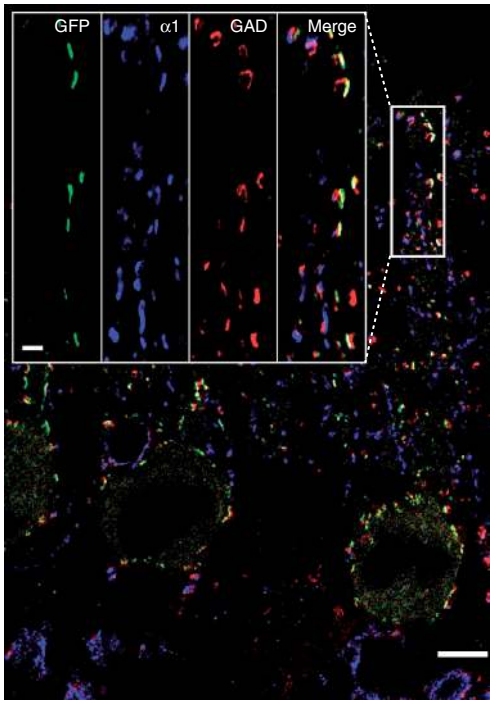

Restriction of zolpidem sensitivity to Purkinje cells

To determine the zolpidem sensitivity of GABAergic synaptic transmission in the different mouse lines, we recorded mIPSCs from Purkinje cells and molecular layer interneurons (presumptive stellate cells) in slices prepared from adult mice. As reported previously[22], the properties (amplitude, rise time and decay) of mIPSCs in γ2I77 mice were similar to those of mIPSCs in *γ2F77/F77* and C57BL/6 mice, confirming that the γ2F77I point mutation was a neutral substitution. The *γ2I77lox* mice generated here differ from previously reported *γ2F77I* mice[22] only by the inclusion of a *lox*P site located 5′ to exon 4 (**Supplementary Fig. 1**). Accordingly, mIPSCs recorded in both Purkinje cells (amplitude, 57.5 ± 5.2 pA; 10–90% rise time, 296 ± 11 μs; decay (τ_w; see **Supplementary Methods**), 2.7 ± 0.2 ms; charge transfer, 165.4 ± 13.8 fC; $n = 11$ cells) and stellate cells (61.3 ± 10.4 pA; 328 ± 16 μs; 2.6 ± 0.1 ms; 194.4 ± 33.3 fC; $n = 5$) had properties similar to those of the corresponding mIPSCs reported previously[22].

In situ hybridization data suggested that our Cre-*lox*P strategy eliminated the γ2 subunit from Purkinje cells, a condition necessary to facilitate the Ile77 to Phe77 swap (**Fig. 2**). To confirm this elimination, we also recorded from Purkinje cells of *PC-Δγ2* mice and their *γ2I77lox/γ2I77lox* littermates. Whereas mIPSCs were present in every control Purkinje cell ($n = 21$), they were absent from all Purkinje cells of *PC-Δγ2* mice ($n = 10$; **Fig. 4a**), verifying the effective deletion of the γ2 subunit and the elimination of fast GABAergic synaptic input onto Purkinje cells.

Figure 3 Synaptic expression of the $\gamma2F77^{GFP}$ subunit in Purkinje cells of adult *PC-γ2–swap* mice. A confocal microscopic image shows immunoreactivity for GFP (green), the α1 subunit of the $GABA_A$ receptor (blue) and GAD (red) in the cerebellum. Note the short segments of GFP immunoreactivity surrounding the somata and dendrites of Purkinje cells. Glomeruli in the granule cell layer are immunonegative for GFP. Inset shows magnified images of the boxed area, indicating that individual GFP patches also contain α1 subunit immunoreactivity and are apposed to GAD-immunoreactive structures corresponding to GABAergic nerve terminals. Other GAD-positive structures apposed to α1 subunit immunoreactive segments represent GABAergic terminals that innervate interneuron (stellate/basket cell) dendrites. Scale bars, 15 μm and 2 μm (inset).

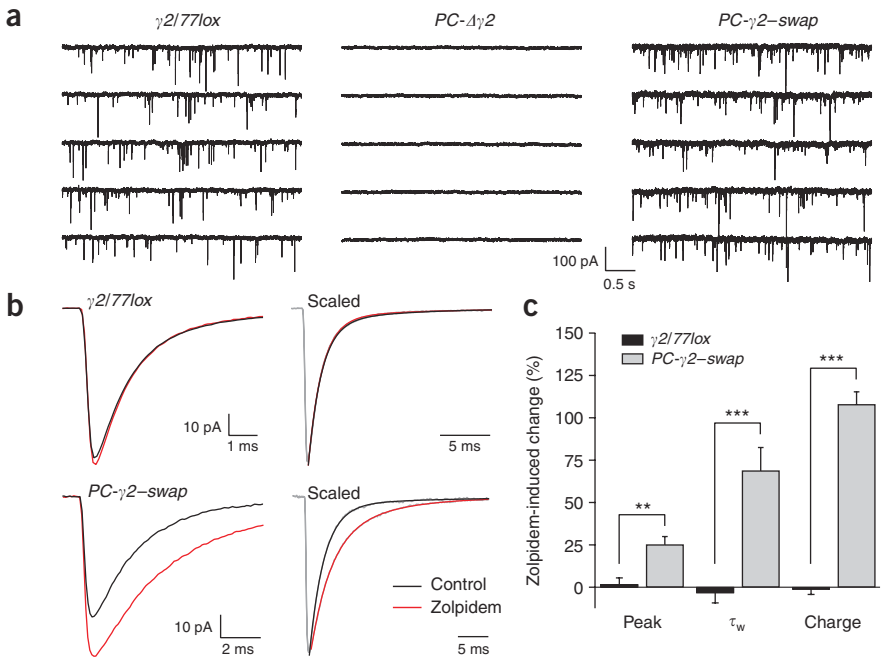

Figure 4 Potentiation of $GABA_A$ receptor–mediated mIPSCs by zolpidem in Purkinje cells of *PC-γ2–swap* mice. (**a**) Continuous 20-s segments of whole-cell recordings (−70 mV) from Purkinje cells of *γ2I77lox* (postnatal day 140), *PC-Δγ2* (P109) and *PC-γ2–swap* (P134) mice. mIPSCs (downward current deflections) are absent from the *PC-Δγ2* recording, but appear normal in the *PC-γ2–swap* recording. (**b**) Superimposed averaged mIPSCs in the absence (black) and presence (red) of zolpidem in *γ2I77lox* (top) and *PC-γ2–swap* (bottom) mice, before (left) and after (right) peak scaling (same cells as in **a**). Smooth red or black lines on the decaying phase of the scaled traces (gray) are fits of double-exponential functions. Zolpidem (1 μM) increased the amplitude and decay of the mIPSCs recorded from the *PC-γ2–swap* Purkinje cell, but had no effect on those recorded from the *γ2I77lox* cell. (**c**) Pooled data showing the effect of zolpidem on peak amplitude, τ_w and charge transfer. Columns indicate means and vertical error bars indicate s.e.m. (**$P < 0.01$, ***$P < 0.001$, Mann Whitney *U*-test; $n = 8$ and 5 for *γ2I77lox* and *PC-γ2–swap* mice, respectively).

In Purkinje cells of *PC-γ2–swap* mice, mIPSC amplitude (46.4 ± 7.2 pA), 10–90% rise time (307 ± 8 μs), τ_w (3.1 ± 0.2 ms) and charge transfer (158.6 ± 21.7 fC) of mIPSCs ($n = 8$) were not significantly different from their corresponding measures in *γ2I77lox* mice (see above; all $P > 0.05$). These data verify effective deletion of the γ2I77 subunit and its replacement with the $\gamma2F77^{GFP}$ subunit. Although basic mIPSC properties in the two lines were indistinguishable, modulation of mIPSCs by zolpidem was, as predicted, markedly different. Zolpidem had no effect on the amplitude or kinetics of mIPSCs in Purkinje cells of *γ2I77lox* mice; in the *PC-γ2–swap* mice, by contrast, it significantly raised the amplitude (49.7 ± 9.9 to 62.0 ± 12.1 pA), prolonged τ_w (3.2 ± 0.2 to 5.3 ± 0.2 ms) and increased the charge transfer (178.9 ± 29.0 to 377.5 ± 13.6 fC) of Purkinje cell mIPSCs ($n = 5$, all $P < 0.05$; **Fig. 4b,c**). The restoration of zolpidem sensitivity was restricted to Purkinje cells: zolpidem had no effect on the properties of mIPSCs recorded from stellate cells in slices from the same mice (**Supplementary Fig. 4** online).

In female *PC-γ2–swap* mice, transgene expression was mosaic and about 50% of Purkinje cells expressed the transgene. Most probably, the $L7\gamma2F77^{GFP}$ transgene integrated on an X chromosome. Accordingly, some Purkinje cells from females showed a complete lack of mIPSCs (equivalent to that seen in the *PC-Δγ2* mice). In cells where the $\gamma2F77^{GFP}$ transgene was expressed, however, mIPSCs were normal and showed zolpidem sensitivity comparable to that of mIPSCs in *γ2F77/F77* or C57BL/6 mice[22]. In male mice, at least 90% of Purkinje cells swapped their γ2 subunits, and only male mice were used for behavioral tests involving zolpidem.

Dynamic modulation of inhibition produces motor deficits

What role does GABAergic inhibition of Purkinje cells have in motor coordination? Unexpectedly, mice with no fast synaptic inhibition onto Purkinje cells (*PC-Δγ2* mice) had no motor disabilities and showed neither ataxia nor tremor. They performed the rotarod task to the same standard as their littermate controls (**Fig. 5a**). Given this observation, we considered what would be the behavioral effect of acute modulation of fast GABAergic input onto Purkinje cells when *PC-γ2–swap* mice were given zolpidem. Without drugs, *PC-γ2–swap* mice showed no motor disabilities: they learned the rotarod task to the same standard as their littermate controls. On the first day of training, a small difference in latency to fall was detected, but this difference disappeared during subsequent training days (**Fig. 5a**).

Intraperitoneal administration of zolpidem to *PC-γ2–swap* mice produced no sedative or overt ataxic effect. Within 1–5 min of drug injection, mice were tested on the rotarod. Zolpidem significantly reduced the ability of trained *PC-γ2–swap* mice to stay on the rotating rod (**Fig. 5b**; repeated measures analysis of variance (ANOVA), $F_{1,84} = 10.4$, $P < 0.001$; zolpidem treatment × mouse line interaction, $F_{1,84} = 47.6$, $P < 0.001$; Newman-Keuls post hoc test, $P < 0.001$). With the initial dose of 3 mg/kg (body weight) of zolpidem, the effect was highly significant (**Fig. 5b**) and almost saturated. No greater effect was produced by a cumulative dose of 9 mg/kg of zolpidem. In an additional experiment, a single dose of 12 mg/kg of zolpidem shortened the latency to fall in the *PC-γ2–swap* mice from 144 ± 30 s to 96 ± 48 s ($P < 0.05$), indicating that the lowest doses used produced the maximal motor-impairing effect. These effects of zolpidem were produced without sedation. This observation was expected, because the γ2I77 subunit, retained in all cells other than Purkinje cells, prevents the normal effects of zolpidem on, for example, sleep regulating centers[13,22]. The *γ2I77lox* littermates were all unaffected.

To further test fine motor coordination and balance, we used the 'walking beam' test, whereby mice have to cross a suspended rod. Without zolpidem, there were no differences between *PC-γ2–swap* mice and their *γ2I77lox* littermates (repeated measures ANOVA, $F_{1,148} = 2.01$, $P > 0.05$, data not shown). After administration of zolpidem (12 mg/kg), however, *PC-γ2–swap* mice needed significantly more time to traverse the beam (treatment × mouse line interaction, repeated measures ANOVA, $F_{1,26} = 9.84$, $P < 0.01$; Newman-Keuls post hoc test, $P < 0.001$ for mouse line). By contrast, their *γ2I77lox* littermates were not affected (**Fig. 5c**).

The behavioral effects produced by zolpidem in *PC-γ2–swap* mice could be blocked by flumazenil (Ro 15-1788), which antagonizes

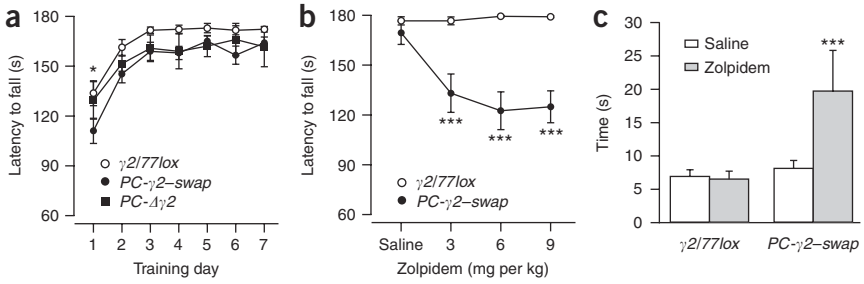

Figure 5 Motor performance on a rotarod and horizontal beam after systemic administration of zolpidem. (**a**) The rotarod was accelerated from 5 to 30 r.p.m. over 180 s. Data for *γ2/77lox* littermate control ($n = 20$), *PC-γ2–swap* ($n = 20$) and *PC-Δγ2* ($n = 5$) mice are presented as the daily means ± s.e.m. of six trials for males and females combined (*$P < 0.05$ for *PC-γ2–swap* versus *γ2/77lox* control mice on training day 1, repeated measures ANOVA and Newman-Keuls post hoc tests). (**b**) Effects of zolpidem on motor performance. Shown is the effect of cumulative doses (3+3+3 mg/kg i.p., total 9 mg/kg) of zolpidem on the rotarod performance of *γ2/77lox* control ($n = 9$) and *PC-γ2–swap* ($n = 5$) male mice. The rotarod was accelerated from 5 to 30 r.p.m. over 180 s (***$P < 0.001$ between mouse lines and $P < 0.001$ versus saline injection within the *PC-γ2–swap* line, one-way ANOVA and Newman-Keuls post hoc tests). Data are presented as means ± s.e.m. (**c**) Effect of 12 mg/kg of i.p. zolpidem on the walking beam performance of *γ2/77lox* control ($n = 9$) and *PC-γ2–swap* ($n = 5$) male mice. Mice were pre-trained for 4 d to traverse the 100-cm long, 0.8-cm diameter wooden beam. Columns represent means and vertical error bars s.e.m. (***$P < 0.001$ between mouse lines and $P < 0.001$ versus saline injection within the *PC-γ2–swap* line, two-way ANOVA and Newman-Keuls post hoc tests).

the binding of zolpidem to $GABA_A$ receptors containing the γ2F77 subunit[24]. *PC-γ2–swap* mice were pre-treated with vehicle or 15 mg/kg of flumazenil and then given a single dose of 6 mg/kg of zolpidem. Immediately afterwards they were tested on the rotarod. The latency to fall in the vehicle pre-treated group ($n = 6$) shortened from 173 ± 13 s to 137 ± 13 s (one-way ANOVA and Newman-Keuls post hoc test, $P < 0.05$), but stayed the same in the group pre-treated with flumazenil (170 ± 13 s; one-way ANOVA, $P > 0.05$ $n = 4$).

DISCUSSION

Rapid modulation avoids adaptational change

Motor coordination on the accelerating rotarod is a complex task, involving many brain areas, cell types and synapses. Here, to demonstrate the feasibility of a reversible method for manipulating defined synapses, we have isolated the contribution of $GABA_A$ receptor–mediated synaptic input onto Purkinje cells to this task. Dynamically modifying GABAergic input, through acute systemic administration of zolpidem to *PC-γ2–swap* mice, produced a result different from that of static long-term removal of the input (through knockout of synaptic $GABA_A$ receptors in *PC-Δγ2* mice). Under the same test conditions, static deletion did not reduce performance on the rotarod, whereas fast and reversible enhancement of the same GABAergic input produced acute debilitating effects. These contrasting results reflect, in the chronic intervention, the adaptive abilities of neurons and networks to engage alternative strategies to achieve similar ends (for example, see refs. 4,35,36). Nevertheless, chronic interventions can be informative. When no compensation occurs, ablating a component can demonstrate its necessity for a particular process. Indeed, *PC-Δγ2* mice do have profound deficits in the consolidation of cerebellar motor memories, indicating that fast inhibition onto Purkinje cells provides essential functions that cannot be compensated for after chronic ablation (P. Wulff *et al.*, unpublished data). Thus, pursuing both types of study (chronic ablation and reversible intervention) gives a fuller picture of how a 'component' (here, a defined synaptic input to a target cell) contributes to a 'system' (here, cerebellar motor coordination).

Several methods to study network components, using either fast (millisecond) or relatively slow (hours to days) interventions, are available. Light-activated ion channels, receptors or pumps enable ultrafast pinpoint activation or inhibition of neurons[37,38]. Although excellent for use *in vitro* or *in vivo* for transparent species, these approaches are likely to be less applicable to the study of behavior and distributed populations of cells *in vivo* in mammals. The *Drosophila* allatostatin receptor system, which couples to mammalian potassium GIRK channels, allows reversible silencing of neurons within seconds and, like light-activated channels, is not limited to a particular vertebrate species[39,40]. The agonist peptide allatostatin, however, requires intracerebral injection and its uneven diffusion in the brain may cause difficulties for *in vivo* studies. Methods that block synaptic transmission have very slow kinetics[41,42], but these approaches seem to be useful for long-term (days) synaptic silencing[41,42]. By contrast, our strategy does not silence or activate cells. Instead, it confers the ability to modulate reversibly the action of an endogenous neurotransmitter and thus it more subtly interferes with network function. These various methods are complementary, potentially enabling a full range of physiological processes to be investigated.

We have shown that zolpidem, by promoting a restricted and specific increase in fast GABAergic inhibition from molecular layer interneurons onto Purkinje cells, decreases the ability of mice to carry out complex motor tasks. To gauge the success of the strategy, it is important to know the extent of motor deficit that one might expect to see after such Purkinje cell–specific modulation. Zolpidem is a potent hypnotic, acting on $GABA_A$ receptors in brain areas that regulate sleep[13]. We have shown previously that in wild-type mice zolpidem produces severe sedation and deficits in rotarod performance[22]; given this sedation, we cannot estimate what fraction of the performance deficit originates from modulation of the cerebellum and motor centers. However, comparable data from studies on benzodiazepine-insensitive mice, notably α1H101R mice, are available. In cerebellar circuits α1βγ2 is the predominant $GABA_A$ receptor type[29,30], and in a wild-type cerebellum zolpidem will modulate IPSCs onto most cell types. From studies of mice (α1H101R) with α1βγ2 receptors made insensitive to diazepam[12,14,15], the net 'contribution' of modulating α1βγ2-type $GABA_A$ receptors to rotarod behaviors (as judged by decreased latencies to fall) is about 25% (this reflects modulation of α1 receptors throughout the brain, not just in the cerebellum[14,15]). We found here that zolpidem, acting on α1βγ2 receptors in Purkinje cells alone, induced a 33% decrease in latency to fall, broadly fitting with results from α1H101R mice[14,15]. The effects seem to be greater than those obtained after blockade of GABA release from Purkinje cell terminals in the deep cerebellar nuclei (15% decrease in latency to fall with the rod rotating at 80 r.p.m.; ref. 41).

Methodological considerations

Our approach is designed to enable zolpidem, through the cell type–selective modulation of $GABA_A$ receptor–mediated synaptic currents,

to be used in behaving animals to alter the activity of defined neuronal populations. For this strategy, active GABAergic synapses are needed. The method requires that targeted neurons express α1, α2 or α3 subunits together with any β subunit and the γ2 subunit. Many cell types do indeed express predominantly α1βγ2- or α2βγ2-type receptors; for example, various subtypes of hippocampal GABAergic interneuron have zolpidem-sensitive $GABA_A$ receptors[10,23]. In Purkinje cells, zolpidem modulation primarily affects synaptic inhibition[22]; these cells do not show a tonic $GABA_A$ receptor–mediated current[30,43]. Other cell types, however, may express zolpidem-sensitive extrasynaptic $GABA_A$ receptors (containing α1, α2 or α3, β and γ2 subunits) with GABA-dependent or GABA-independent tonic activity[7,44]. If such cells were targeted by our strategy, the activity of these receptors would also be enhanced by zolpidem.

Zolpidem can be used both in slices and in behaving animals; it can be administered by intraperitoneal (i.p.) injection or by stereotaxic injection into the brain. Zolpidem binds preferentially to α1-containing $GABA_A$ receptors (α1β2γ2 or α1β3γ2; inhibition constant, $K_i = 20$ nM), but at higher concentrations it will modulate receptors containing α2 or α3 subunits (α2βγ2 or α3βγ2; $K_i = 400$ nM). Because zolpidem can be given at doses of up to 30 mg/kg in *γ2I77* mice with no effects[22], it can be used to modulate cell types that express only α2- and α3-containing $GABA_A$ receptors. Zolpidem tartrate is the preferred preparation because of its maximal water solubility. An advantage of our method is that zolpidem has a rapid and short-acting effect: zolpidem maximally occupies its binding sites in mouse brain within minutes of i.p. injection and has a half-life of 20 min (ref. 45).

In addition to zolpidem, various other $GABA_A$ receptor modulatory drugs, such as the β-carbolines DMCM and β-CCM, the imidazobenzodiazepine bretazenil, the cyclopyrrolone zopiclone, and the quinolines PK 8165 and PK 9084, depend on the Phe77 residue of the γ2 subunit for binding[20,21,24]. On neuronal membranes isolated from *γ2I77* mouse brains, the binding affinities of these drugs are greatly reduced[24]. Some of these drugs, for example DMCM and β-CCM, are inverse agonists at the benzodiazepine binding site of $GABA_A$ receptors and decrease receptor function[11,20,21]. The usual effect of DMCM administration (seizures) is abolished in *γ2I77* mice[46]. Thus, in principle, both zolpidem and an inverse agonist can be used to bidirectionally modulate fast inhibition onto neurons that have undergone a γ2 subunit swap.

For its full potential to be realized, the method that we describe will require mouse Cre lines with suitable cell type–specific expression. The brain region– and cell type–specific gene expression patterns identified in, for example, the Allen Brain Atlas project will eventually aid this aim[47]. We used triple crosses of mouse lines, but the procedure could be streamlined by using Cre-mediated switching of an Ile77 to a Phe77 exon or viral delivery of a *γ2F77-ires-Cre* transgene into *γ2I77lox* brains. We anticipate that the unique features of our method will be invaluable for investigating the contribution of specific neurons to brain function and behavior.

METHODS

Transgenic mouse production and breeding. All procedures were done in accordance with the United Kingdom Animals (Scientific Procedures) Act 1986, had ethical approval from the Regierungspräsidium Karlsruhe or were approved by the Laboratory Animal Committee of the University of Helsinki.

Production of the *γ2I77lox* and *L7γ2F77*^{GFP} lines and mouse genotyping are described in the **Supplementary Methods**. Mice homozygous for the *γ2I77lox* gene and heterozygous for the *L7γ2F77*^{GFP} transgene were crossed with mice homozygous for *γ2I77lox* and heterozygous for an *L7Cre* transgene[33]. Littermates of the following genotypes were used for the experiments: *γ2I77lox/γ2I77lox/L7γ2*^{GFP}*/L7Cre* (*PC-γ2–swap*), *γ2I77lox/γ2I77lox/L7Cre* (*PC-Δγ2*) and γ2I77lox/γ2I77lox (littermate controls).

***In situ* hybridization.** We carried out *in situ* hybridization as described[16]. The probe sequences to exon 4 of the γ2 subunit and *GFP* are given in the **Supplementary Methods**.

Triple labeling immunohistochemistry. We used the following primary antibodies: affinity-purified rabbit antibody to the α1 subunit[48] (0.5 μg/ml), guinea-pig antiserum to EGFP (1:100; a gift from R. Tomioka, RIKEN, Japan) and sheep antibody to GAD (1:1,000; ref. 49). See **Supplementary Methods** for detailed protocol and image acquisition.

Electrophysiology. Whole-cell recordings were made from neurons in parasagittal slices of cerebellar vermis prepared from adult male and female mice. A bicarbonate-buffered 'external' solution and a CsCl-based 'internal' solution (near symmetrical Cl^- concentration) were used. mIPSCs were recorded at −70 mV in the presence of 5 μM CNQX (6 cyano-7-nitroquinoxaline-2,3-dione disodium), 10 μM D-AP5 and 0.5–1.0 μM tetrodotoxin. In all tests, synaptic currents recorded under such conditions were completely blocked by the $GABA_A$ receptor antagonist SR 95531 (gabazine, 10–20 μM; data not shown). All recordings were made at near physiological temperature (34–38 °C), except those from *PC-Δγ2* mice and their littermates, which were made at room temperature (22–25 °C). For full details of the recording and analysis, see **Supplementary Methods**.

Zolpidem (Tocris Bioscience) was dissolved in dimethyl sulfoxide (DMSO) at a concentration of 50 mM and was used at 1 μM (final DMSO 0.002%). Zolpidem was applied to each slice only once, and its effect on mIPSCs was determined only after equilibration for at least 2 min.

Statistical tests were done with GraphPad Prism software (Prism 3.0, GraphPad Software Inc.). Except where noted, treatment groups and mouse lines were compared with two-tailed paired or unpaired Student's *t*-tests, as appropriate. Where data were non-normally distributed (Shapiro-Wilk test), non-parametric tests were used (Wilcoxon Matched pairs or Mann-Whitney U-test). The level of significance was set at $P < 0.05$.

Mouse behavioral experiments. Male and female *γ2I77lox* ($n = 20$; all bred as littermates from the compound crosses, see above), *PC-γ2–swap* ($n = 20$) and *PC-Δγ2* ($n = 5$) mice aged 4–10 months (20–45 g) were used in tests. Basic behavioral characterization was done as described in the **Supplementary Methods**.

Rotarod and horizontal beam tests were done as described[50]. The mice were given an i.p. injection of zolpidem (Sanofi-Synthelabo AB) 1–5 min before the rotarod and walking beam tests (1–4 trials). Zolpidem tartrate was crushed from a tablet, suspended in physiological saline and injected at 10 ml/kg (body weight). Drug dosing was either acute (one bolus injection) or cumulative (3 plus 3 plus 3 mg/kg, 5 min between injections). We used cumulative dosing of zolpidem with repeated rotarod testing in male mice. There was a minimum washout period of 3 d between pharmacological tests. Full details are given in the **Supplementary Methods**.

Statistical analyses of motor behavior were performed with SPSS 12.0.1 (SPSS Inc.) or GraphPad Prism software. Treatment groups and mouse lines were compared with either repeated measures ANOVA or one-way ANOVA, followed by Newman-Keuls post hoc test or Dunnett's test. In all statistical tests, the significance level was set at $P < 0.05$.

Note: Supplementary information is available on the Nature Neuroscience website.

ACKNOWLEDGMENTS

We thank E. Sigel for pointing out the γ2I77 mutation; J. Oberdick for the L7 expression cassette; S.J. Moss for the γ2F77^{GFP} plasmid; M. Meyer for the *L7Cre* line; R. Tomioka and E. Mugnaini for antibodies to EGFP and GAD, respectively; H. Monyer for discussion and support; F. Zimmermann for the transgene and stem cell injections; I. Preugschat-Gumprecht for help with mouse genotyping; D. Andersson, T. Karayannis and M. Capogna for contributing to initial electrophysiological recordings; and S. Brickley, M. Capogna, S.G. Cull-Candy, C. De Zeeuw, N. Franks, T. Klausberger and Z. Nusser for comments on the manuscript. This work was funded by the VolkswagenStiftung (grant I/78 554 to W.W., E.R.K., W.S. and P.S.), the Deutsche Forschungsgemeinschaft

(grant WI 1951/2 to W.W. and P.W.), the UK Medical Research Council (grant G0501584 to W.W.), the J. Ernest Tait Estate (to W.W. and T.G.), a Heidelberg Young Investigator Award (to P.W.), the Academy of Finland (to E.R.K. and A.-M.L.), the Sigrid Juselius Foundation (to E.R.K. and E.L.), the Institute Pasteur-Fondazione Cenci Bolognetti (to M.R.), the Austrian Federal Government (W.S.), the Medical University Vienna (W.S.) and a Wellcome Trust Programme Grant (to M.F.).

AUTHOR CONTRIBUTIONS

The original idea was conceived by W.S. and developed with P.S., W.W. and E.R.K. Experiments were designed by M.F., E.R.K., P.S., P.W., W.S. and W.W. Experiments were performed by M.F., T.G., A.-M.L., E.L., M.R., J.D.S., P.S., O.Y.V., P.W. and W.W. Behavioral data were analyzed by E.L., A.-M.L. and E.R.K. Electrophysiological data were analyzed by M.F. The manuscript was written by M.F., P.W. and W.W. All authors commented on and helped to revise the text.

COMPETING INTERESTS STATEMENT

The authors declare no competing financial interests.

Published online at http://www.nature.com/natureneuroscience
Reprints and permissions information is available online at http://npg.nature.com/reprintsandpermissions

1. Riedel, G. *et al.* Reversible neural inactivation reveals hippocampal participation in several memory processes. *Nat. Neurosci.* **2**, 898–905 (1999).
2. Lomber, S.G. The advantages and limitations of permanent or reversible deactivation techniques in the assessment of neural function. *J. Neurosci. Methods* **86**, 109–117 (1999).
3. Pereira de Vasconcelos, A. *et al.* Reversible inactivation of the dorsal hippocampus by tetrodotoxin or lidocaine: a comparative study on cerebral functional activity and motor coordination in the rat. *Neuroscience* **141**, 1649–1663 (2006).
4. Wulff, P. & Wisden, W. Dissecting neural circuitry by combining genetics and pharmacology. *Trends Neurosci.* **28**, 44–50 (2005).
5. Crick, F. The impact of molecular biology on neuroscience. *Phil. Trans. R. Soc. Lond. B* **354**, 2021–2025 (1999).
6. Rudolph, U. & Mohler, H. Analysis of $GABA_A$ receptor function and dissection of the pharmacology of benzodiazepines and general anesthetics through mouse genetics. *Annu. Rev. Pharmacol. Toxicol.* **44**, 475–498 (2004).
7. Farrant, M. & Nusser, Z. Variations on an inhibitory theme: phasic and tonic activation of $GABA_A$ receptors. *Nat. Rev. Neurosci.* **6**, 215–229 (2005).
8. Whiting, P.J. $GABA_A$ receptors: a viable target for novel anxiolytics? *Curr. Opin. Pharmacol.* **6**, 24–29 (2006).
9. Perrais, D. & Ropert, N. Effect of zolpidem on miniature IPSCs and occupancy of postsynaptic $GABA_A$ receptors in central synapses. *J. Neurosci.* **19**, 578–588 (1999).
10. Thomson, A.M., Bannister, A.P., Hughes, D.I. & Pawelzik, H. Differential sensitivity to Zolpidem of IPSPs activated by morphologically identified CA1 interneurons in slices of rat hippocampus. *Eur. J. Neurosci.* **12**, 425–436 (2000).
11. Campo-Soria, C., Chang, Y. & Weiss, D.S. Mechanism of action of benzodiazepines on $GABA_A$ receptors. *Br. J. Pharmacol.* **148**, 984–990 (2006).
12. Rudolph, U. *et al.* Benzodiazepine actions mediated by specific γ-aminobutyric $acid_A$ receptor subtypes. *Nature* **401**, 796–800 (1999).
13. Crestani, F., Martin, J.R., Mohler, H. & Rudolph, U. Mechanism of action of the hypnotic zolpidem *in vivo*. *Br. J. Pharmacol.* **131**, 1251–1254 (2000).
14. Crestani, F., Martin, J.R., Mohler, H. & Rudolph, U. Resolving differences in $GABA_A$ receptor mutant mouse studies. *Nat. Neurosci.* **3**, 1059 (2000).
15. McKernan, R.M. *et al.* Sedative but not anxiolytic properties of benzodiazepines are mediated by the $GABA_A$ receptor α1 subtype. *Nat. Neurosci.* **3**, 587–592 (2000).
16. Wisden, W., Laurie, D.J., Monyer, H. & Seeburg, P.H. The distribution of 13 $GABA_A$ receptor subunit mRNAs in the rat brain. I. Telencephalon, diencephalon, mesencephalon. *J. Neurosci.* **12**, 1040–1062 (1992).
17. Duncan, G.E. *et al.* Distribution of [^{3}H]zolpidem binding sites in relation to messenger RNA encoding the α1, β2 and γ2 subunits of $GABA_A$ receptors in rat brain. *Neuroscience* **64**, 1113–1128 (1995).
18. Niddam, R., Dubois, A., Scatton, B., Arbilla, S. & Langer, S.Z. Autoradiographic localization of [^{3}H]zolpidem binding sites in the rat CNS: comparison with the distribution of [^{3}H]flunitrazepam binding sites. *J. Neurochem.* **49**, 890–899 (1987).
19. Sancar, F., Ericksen, S.S., Kucken, A.M., Teissere, J.A. & Czajkowski, C. Structural determinants for high-affinity zolpidem binding to $GABA_A$ receptors. *Mol. Pharmacol.* **71**, 38–46 (2007).
20. Buhr, A., Baur, R. & Sigel, E. Subtle changes in residue 77 of the γ subunit of $\alpha1\beta2\gamma2$ $GABA_A$ receptors drastically alter the affinity for ligands of the benzodiazepine binding site. *J. Biol. Chem.* **272**, 11799–11804 (1997).
21. Wingrove, P.B., Thompson, S.A., Wafford, K.A. & Whiting, P.J. Key amino acids in the γ subunit of the γ-aminobutyric $acid_A$ receptor that determine ligand binding and modulation at the benzodiazepine site. *Mol. Pharmacol.* **52**, 874–881 (1997).
22. Cope, D.W. *et al.* Abolition of zolpidem sensitivity in mice with a point mutation in the $GABA_A$ receptor γ2 subunit. *Neuropharmacology* **47**, 17–34 (2004).
23. Cope, D.W. *et al.* Loss of zolpidem efficacy in the hippocampus of mice with the $GABA_A$ receptor γ2 F77I point mutation. *Eur. J. Neurosci.* **21**, 3002–3016 (2005).
24. Ogris, W. *et al.* Affinity of various benzodiazepine site ligands in mice with a point mutation in the $GABA_A$ receptor γ2 subunit. *Biochem. Pharmacol.* **68**, 1621–1629 (2004).
25. Smeyne, R.J. *et al.* Local control of granule cell generation by cerebellar Purkinje cells. *Mol. Cell. Neurosci.* **6**, 230–251 (1995).
26. Häusser, M. & Clark, B.A. Tonic synaptic inhibition modulates neuronal output pattern and spatiotemporal synaptic integration. *Neuron* **19**, 665–678 (1997).
27. Mittmann, W., Koch, U. & Häusser, M. Feed-forward inhibition shapes the spike output of cerebellar Purkinje cells. *J. Physiol. (Lond.)* **563**, 369–378 (2005).
28. Santamaria, F., Tripp, P.G. & Bower, J.M. Feed-forward inhibition controls the spread of granule cell-induced Purkinje cell activity in the cerebellar cortex. *J. Neurophysiol.* **97**, 248–263 (2007).
29. Laurie, D.J., Seeburg, P.H. & Wisden, W. The distribution of 13 $GABA_A$ receptor subunit mRNAs in the rat brain. II. Olfactory bulb and cerebellum. *J. Neurosci.* **12**, 1063–1076 (1992).
30. Fritschy, J.M., Panzanelli, P., Kralic, J.E., Vogt, K.E. & Sassoe-Pognetto, M. Differential dependence of axo-dendritic and axo-somatic GABAergic synapses on $GABA_A$ receptors containing the α1 subunit in Purkinje cells. *J. Neurosci.* **26**, 3245–3255 (2006).
31. Gunther, U. *et al.* Benzodiazepine-insensitive mice generated by targeted disruption of the γ2 subunit gene of γ-aminobutyric acid type A receptors. *Proc. Natl. Acad. Sci. USA* **92**, 7749–7753 (1995).
32. Schweizer, C. *et al.* The γ2 subunit of $GABA_A$ receptors is required for maintenance of receptors at mature synapses. *Mol. Cell. Neurosci.* **24**, 442–450 (2003).
33. Barski, J.J., Dethleffsen, K. & Meyer, M. Cre recombinase expression in cerebellar Purkinje cells. *Genesis* **28**, 93–98 (2000).
34. Kittler, J.T. *et al.* Analysis of $GABA_A$ receptor assembly in mammalian cell lines and hippocampal neurons using γ2 subunit green fluorescent protein chimeras. *Mol. Cell. Neurosci.* **16**, 440–452 (2000).
35. Brickley, S.G., Revilla, V., Cull-Candy, S.G., Wisden, W. & Farrant, M. Adaptive regulation of neuronal excitability by a voltage-independent potassium conductance. *Nature* **409**, 88–92 (2001).
36. Marder, E. & Goaillard, J.M. Variability, compensation and homeostasis in neuron and network function. *Nat. Rev. Neurosci.* **7**, 563–574 (2006).
37. Lima, S.Q. & Miesenbock, G. Remote control of behavior through genetically targeted photostimulation of neurons. *Cell* **121**, 141–152 (2005).
38. Zhang, F. *et al.* Multimodal fast optical interrogation of neural circuitry. *Nature* **446**, 633–641 (2007).
39. Gosgnach, S. *et al.* V1 spinal neurons regulate the speed of vertebrate locomotor outputs. *Nature* **440**, 215–219 (2006).
40. Tan, E.M. *et al.* Selective and quickly reversible inactivation of mammalian neurons *in vivo* using the *Drosophila* allatostatin receptor. *Neuron* **51**, 157–170 (2006).
41. Karpova, A.Y., Tervo, D.G., Gray, N.W. & Svoboda, K. Rapid and reversible chemical inactivation of synaptic transmission in genetically targeted neurons. *Neuron* **48**, 727–735 (2005).
42. Yamamoto, M. *et al.* Reversible suppression of glutamatergic neurotransmission of cerebellar granule cells *in vivo* by genetically manipulated expression of tetanus neurotoxin light chain. *J. Neurosci.* **23**, 6759–6767 (2003).
43. Wall, M.J. & Usowicz, M.M. Development of action potential-dependent and independent spontaneous $GABA_A$ receptor-mediated currents in granule cells of postnatal rat cerebellum. *Eur. J. Neurosci.* **9**, 533–548 (1997).
44. McCartney, M.R., Deeb, T.Z., Henderson, T.N. & Hales, T.G. Tonically active $GABA_A$ receptors in hippocampal pyramidal neurons exhibit constitutive GABA-independent gating. *Mol. Pharmacol.* **71**, 539–548 (2007).
45. Benavides, J. *et al. In vivo* interaction of zolpidem with central benzodiazepine (BZD) binding sites (as labeled by [^{3}H]Ro 15–1788) in the mouse brain. Preferential affinity of zolpidem for the omega 1 (BZD1) subtype. *J. Pharmacol. Exp. Ther.* **245**, 1033–1041 (1988).
46. Leppa, E. *et al.* Agonistic effects of the β-carboline DMCM revealed in $GABA_A$ receptor γ2 subunit F77I point-mutated mice. *Neuropharmacology* **48**, 469–478 (2005).
47. Lein, E.S. *et al.* Genome-wide atlas of gene expression in the adult mouse brain. *Nature* **445**, 168–176 (2007).
48. Zezula, J., Fuchs, K. & Sieghart, W. Separation of α1, α2 and α3 subunits of the $GABA_A$-benzodiazepine receptor complex by immunoaffinity chromatography. *Brain Res.* **563**, 325–328 (1991).
49. Oertel, W.H., Schmechel, D.E., Mugnaini, E., Tappaz, M.L. & Kopin, I.J. Immunocytochemical localization of glutamate decarboxylase in rat cerebellum with a new antiserum. *Neuroscience* **6**, 2715–2735 (1981).
50. Korpi, E.R. *et al.* Cerebellar granule-cell–specific $GABA_A$ receptors attenuate benzodiazepine-induced ataxia: evidence from α6-subunit-deficient mice. *Eur. J. Neurosci.* **11**, 233–240 (1999).

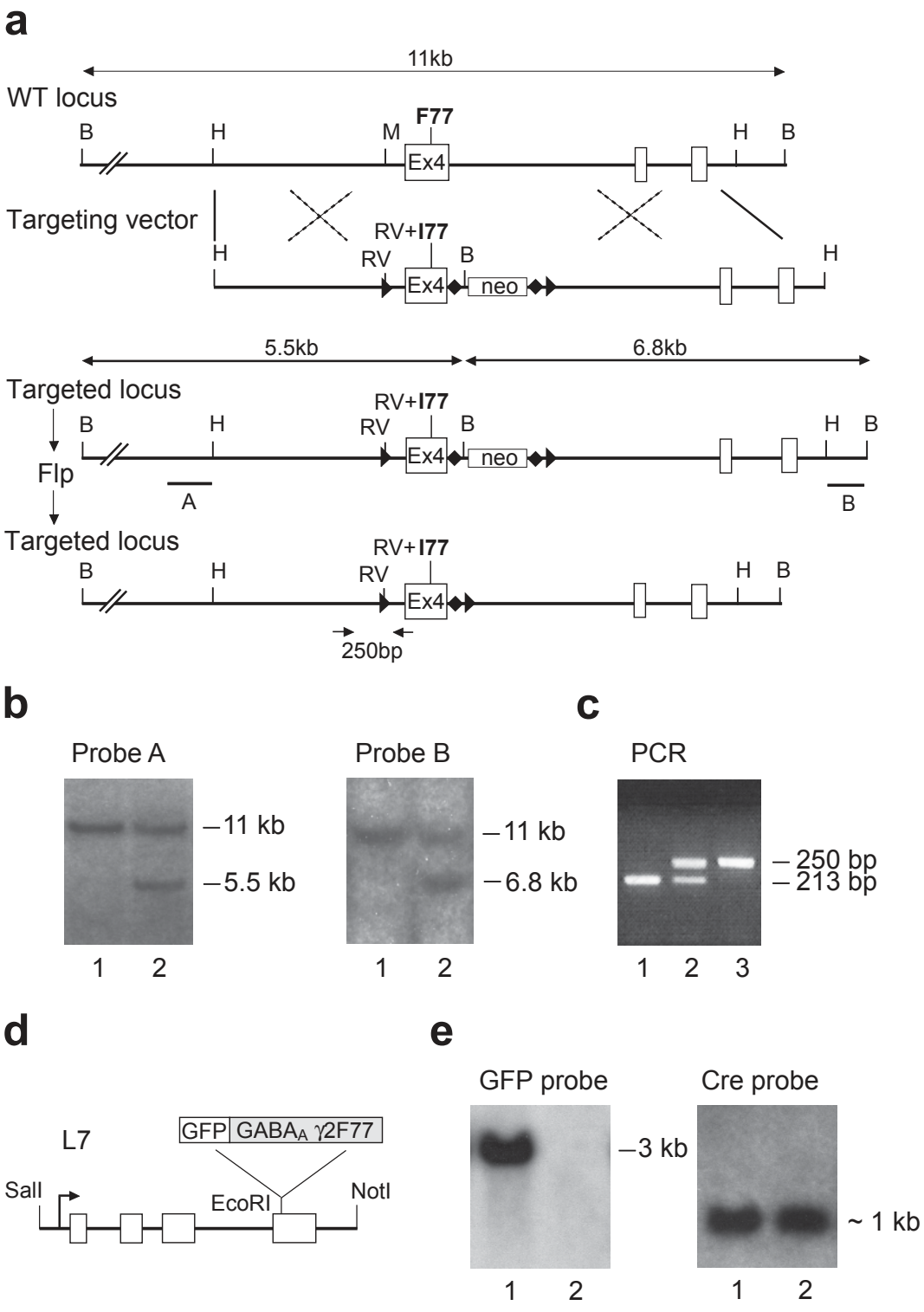

Figure S1 Generation of *γ2I77lox* and *L7γ2F77^{GFP}* mice. *Full legend on following page.*

Figure S1 Generation of *γ2I77lox* and *L7γ2F77^{GFP}* mice. (**a**) Targeting strategy for the generation of *γ2I77lox* mice. A mutation changing the codon of phenylalanine (F) to isoleucine (I) at position 77 was inserted along with an EcoRV (RV) site into the fourth exon (Ex4) of the γ2 subunit gene. A loxP site (black triangle) containing an RV site was inserted into the MscI (M) site in intron 3. For the initial targeting the neomycin resistance cassette (neo) was flanked by two frt sites (black diamonds) and cloned into intron four. The neomycin resistance cassette contains a loxP site at the 3′ end. After gene targeting and germ line transmission mice were mated with a Flp deleter strain to remove the neomycin resistance cassette. Open boxes indicate exons. H indicates HindIII, B indicates BglII restriction sites, black bars labelled A and B indicate the 5′ and 3′ external probes used for Southern blot analysis. Expected fragment sizes of the wild-type and targeted γ2 locus are also indicated. Arrows below the targeted locus indicate PCR primers used for genotyping. The number underneath the arrows indicates the size of the amplified fragment. (**b**) Southern blot analysis of BglII-digested ES cell DNA after gene targeting hybridized with probe A and B respectively. Lane 2 shows a targeted ES cell clone. (**c**) Genotyping of mouse tail DNA by PCR. The amplified fragment of wild-type (lane 1) mice gives rise to a 213 bp band. The loxP site increases the fragment size to 250 bp in heterozygous (lane 2) and homozygous (lane 3) mutant mice. (**d**) *L7γ2F77^{GFP}* transgene construct for the generation of *PC-γ2-swap* mice. The γ2F77^{GFP} reading frame (Supplementary Ref. 3) was cloned into exon 4 of the modified L7ΔAUG-vector (Supplementary Ref. 4). (**e**) Southern blot analysis of EcoRI- (left) and BamHI- (right) digested mouse tail DNA hybridized with probes specific for GFP and Cre recombinase respectively. For each blot, lane 1 shows a *PC-γ2-swap* mouse (positive for γ2F77^{GFP} and Cre), and lane 2 shows a *PC-Δγ2* mouse (positive only for Cre).

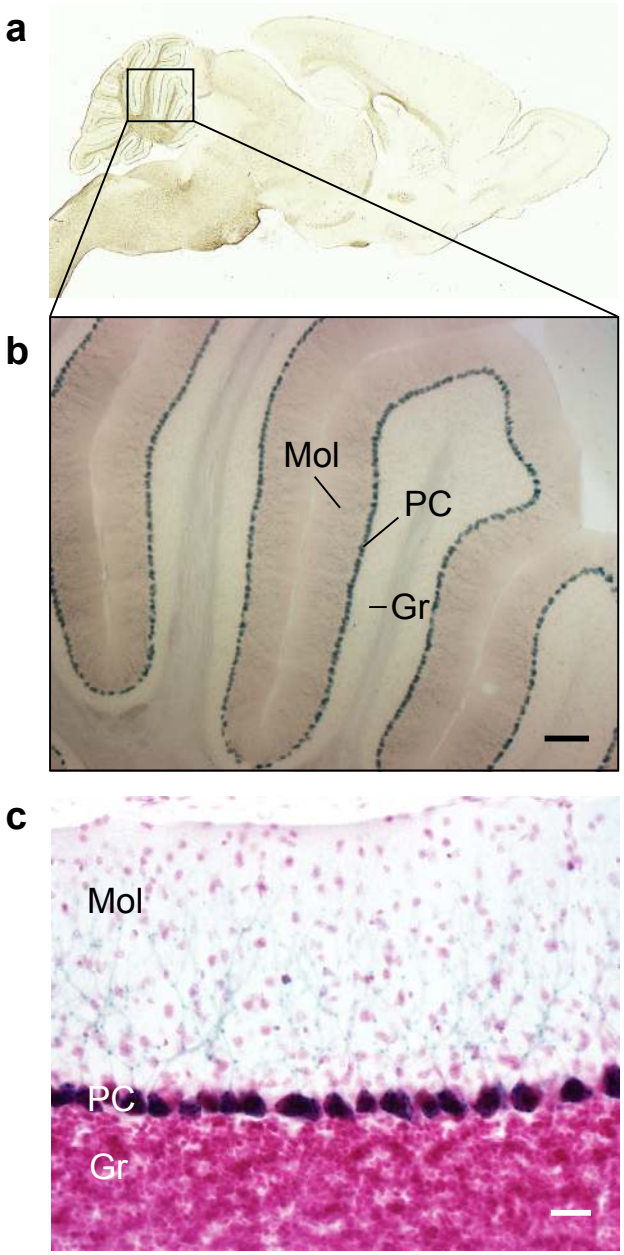

Figure S2 Confirmation of Purkinje cell–specific Cre activity in the *L7Cre* line using *ROSA26* indicator mice. (**a-c**) β-galactosidase staining of sagittal brain sections from *ROSA26* (Supplementary Ref. 8) x *L7Cre* (Supplementary Ref. 9) crosses. (**a**) Cre recombinase activity (blue color) is restricted to cerebellar Purkinje cells. (**b**) Magnification of boxed area in (a). (**c**) Counterstaining with neutral red shows absence of β-galactosidase staining in granule cells and interneurons of the molecular layer. PC, Purkinje cell layer; Mol, molecular layer; Gr, granule cell layer. Scale bar: (b), 125 μm; (c), 50 μm.

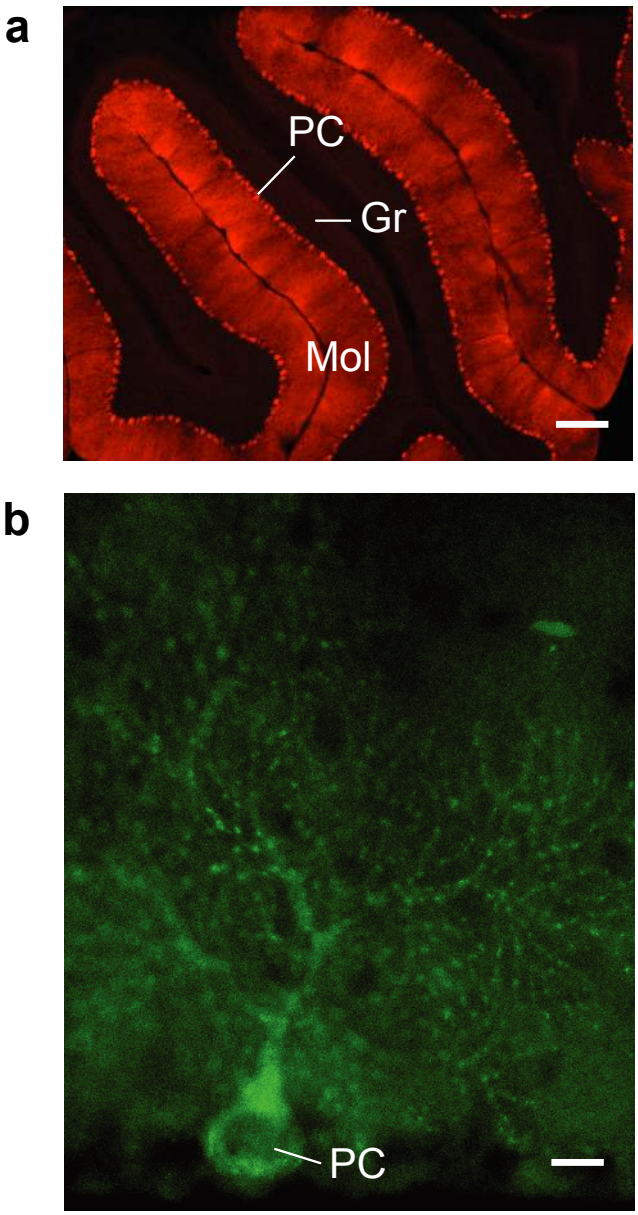

Figure S3 Expression of the γ*2F77*^{GFP} subunit in cerebellar Purkinje cells of *PC-γ2–swap* mice. (**a**) Fluorescent light microscope image showing immunoreactivity for GFP (red) in the molecular (Mol) and Purkinje cell (PC) layers in the cerebellum of an adult *PC-γ2–swap* mouse. The granule cell layer (Gr) is immuno-negative for GFP. (**b**) Fluorescent microscope image showing *native* GFP fluorescence in the soma and dendrites of a Purkinje cell at higher magnification. Note the presence of fluorescent clusters along the dendrites. Scale bar: (a), 125 μm, (b); 15 μm.

Supplementary Methods

1. Generation of *γ2I77lox* mice

γ2I77lox mice were generated as described[1], except that the targeting vector contained a loxP site located 5′ of exon 4 (Fig. S1a). The loxP oligonucleotide, incorporating a 5′ EcoRV site (5′-GATATCCCATAACTTCGTATAGCATACATTATACGAAGTTAT-3′ (the EcoRV site is underlined), was ligated into the MscI site in intron 3. Linearized targeting vector was electroporated into RI embryonic stem cells. Cells were grown on feeder fibroblasts and selected in neomycin-containing medium. Correctly targeted ES cell clones were identified by Southern blot analysis (**Fig. S1b**). One of the positive clones was injected into *C57BL/6* blastocysts. Male chimeras were crossed with deleter mice expressing enhanced-FLP recombinase (Ref 2; Jackson Laboratory) to remove the neomycin resistance cassette. The FLP transgene was bred out by backcrossing to *C57BL/6* mice for 2 generations. Heterozygous mice were then intercrossed to generate homozygous *γ2I77lox* mice. PCR with primers flanking exon 4 and the 5′ loxP sites on genomic DNA from homozygous *γ2I77lox* mice, and sequencing of the products confirmed the presence of the F to I mutation at position 77 in exon 4 and the 5′ loxP site. Mice were genotyped by PCR analysis of genomic DNA from tail biopsies (**Fig. S1c**) using the following primer: γ2lx5′_s (5′-GTCATGCTAAATATCCTACAGTGG-3′) and γ2lx5′_as (5′-GGATAGTGCATCAGCAGACAATAG-3′).

2. The zolpidem-sensitive γ2F77^{GFP} subunit and the generation of *L7γ2F77^{GFP}* transgenic mice

For γ2F77 subunit transgene expression, we used a zolpidem-sensitive $GABA_A$ receptor γ2L subunit that was N-terminally-tagged with EGFP[3], permitting us to distinguish this subunit from the endogenous γ2I77 subunit expression in the *γ2I77lox* brains. The γ2F77^{GFP} construct encodes an N-terminal EGFP fusion with the wild-type mouse γ2L subunit, such that the EGFP reading frame, positioned between amino acids 4 and 5 of the mature γ2 peptide, follows the predicted signal peptide cleavage site; a 9E10 (myc) epitope tag is placed just after the EGFP[3]; "L" denotes the long-splice version of the large cytoplasmic loop of the subunit. This γ2F77^{GFP} subunit was previously demonstrated in HEK cells and for transfected hippocampal neurons in primary culture to assemble into functional $GABA_A$ receptors that were benzodiazepine (diazepam)-sensitive[3]. The properties of this receptor did not differ significantly from untagged recombinant receptors[3].

Three restriction sites in the L7ΔAUG plasmid[4] were modified: The 5′ HindIII site was changed to SalI, the BamHI site in exon 4 was changed to EcoRI, the 3′ EcoRI site was changed to NotI. The *γ2F77^{GFP}* reading frame was cloned into the EcoRI site in exon 4 of the L7 cassette (**Fig. S1d**). The transgene construct was excised from the vector by digestion with SalI/NotI, purified after electrophoresis using GELase (Epicentre Technologies, Madison, WI, USA) and injected at a concentration of 0.3 µg/ml into the pronuclei of *B6D2/F1Crl* x *C57BL/6NCrl* mouse two-cell embryos. One *L7F77γ2^{GFP}* transgenic mouse line with strong and restricted expression of γ2F77^{GFP} in cerebellar Purkinje cells was used in the subsequent breedings. Mice were crossed to *C57BL/6* for 2 generations and then crossed with *γ2I77lox* mice. Mice were genotyped by Southern blot analysis of EcoRI-digested genomic tail DNA hybridized with a probe specific for GFP (**Fig. S1e**). Mice carrying the *L7Cre* transgene were identified by Southern blot analysis of BamHI-digested genomic tail DNA hybridized with a probe specific for Cre recombinase (**Fig. S1e**).

3. *In situ* hybridization

The oligonucleotide sequences used were:

γ2-Ex4: 5′-GTGTCTGGAATCCAGATTTTCCCCACCATATTGCTATTCAAC-3′,

GFP: 5′-ATGCGGTTCACCAGGGTGTCGCCCTCGAACTTCACCTCGGCGCGGGT-3′.

Images were generated from 2 to 4 week exposures to Biomax MR x-ray film (Eastman Kodak, Rochester, NY). To assess non-specific labeling of the sections, each labeled oligonucleotide was hybridized to brain sections with a 100-fold excess of unlabeled oligonucleotide.

4. EGFP immunocytochemistry, EGFP imaging and β-galactosidase staining

For the images in **Fig. S2** and **Fig. S3**, adult mice were transcardially perfused with 4% paraformaldehyde in PBS, pH 7.4. Brains were removed and 60-μm-thick saggital sections were cut using a Leica VT1000S vibratome. Free-floating sections were washed in PBS three times for 10 min, permeabilized in PBS plus 0.4% Triton X-100 for 30 min, blocked by incubation in PBS plus 4% normal goat serum (NGS), 0.2% Triton X-100 for 30 min (all at room temperature) and subsequently incubated with a rabbit polyclonal anti-EGFP (1/1000 dilution, Molecular Probes) primary antibody in a solution composed of 2% NGS, 0.1% Triton X-100 in PBS for 24 h at 4°C. Incubated slices were washed three times in PBS plus 1% NGS for 10 min at room temperature, incubated for 2 h at room temperature with a 1:800 dilution of a Cy3-conjugated goat anti-rabbit IgG (Jackson ImmunoResearch) in PBS plus 1.5% NGS, and subsequently washed twice in PBS plus 1% NGS and twice in PBS alone for 10 min at room temperature. Slices were rinsed briefly in 10 mM TRIS-HCl, mounted on slides, embedded in Mowiol, cover-slipped, and analyzed using an upright fluorescent microscope (Zeiss Axioplan 2; Zeiss) equipped with a Zeiss filter set 10 for detection of EGFP (excitation filter BP 450–490; dichroic mirror FT 510; emission filter BP 515–565) and filter set 15 for detection of Cy3 (excitation filter BP 546/12; dichroic mirror FT 580; emission filter LP 590).

For β-galactosidase staining (**Fig. S2**), 60 μm free-floating sections were incubated in 5-bromo-4-chloro-3-indolyl-β-galactoside (X-Gal) for 30-60 min[5]. After X-Gal staining some sections were counterstained with neutral red (Sigma).

5. Immunocytochemistry: triple labeling

5.1 EGFP, GAD and α1 subunit labeling. Two female *PC-γ2–swap* mice and two wild-type control littermates were deeply anaesthetised with a mixture of fentanyl citrate and midazolam hydrochloride dissolved in sterile water (1:1:2 ratio, respectively, i.p., 0.1 ml per 10 g). Animals were perfused transcardially with saline followed by a fixative composed of 2% paraformaldehyde, ~0.2% picric acid in 0.1 M phosphate buffer (PB, pH 7.2-7.4) for 15 min. After perfusion, the brains were removed, rinsed extensively in PB, and sectioned in the sagittal or frontal planes on a vibratome at 70 μm thickness. For triple-immunofluorescence, free-floating sections were incubated in blocking solution of 20% normal donkey serum (NDS) diluted in tris buffered saline (TBS, pH 7.4, 0.3% Triton) for 1 hour. The sections were then incubated in the following cocktail of primary antibodies overnight at 4° C: affinity purified rabbit antibody (0.5 μg/ml) to the α1 subunit (see **Methods**), guinea pig antiserum to EGFP (1:100, a gift from Dr Ryohei Tomioka, RIKEN, Japan) and sheep antibody to GAD (1:1000, see **Methods**). The following day, the sections were rinsed thoroughly in TBS and then incubated in a cocktail containing donkey anti-rabbit Cy5 (1:250, Jackson ImmunoResearch), donkey anti-sheep Cy3 (1:300, Jackson ImmunoResearch), and donkey anti-guinea pig Alexa 488 (1:1000, Invitrogen) for 2 hours at room temperature. Finally, the sections were rinsed in PB and mounted in Vectashield (Vector Laboratories, Burlingame, CA). Antibody specificity is described in the cited papers. For method specificity, sections were incubated in one primary antibody with the full set of three secondary antibodies and images were acquired at all wavelengths. No cross-reactivity was found.

5.2 Image acquisition. Twelve-bit, 1024x1024 pixel images were acquired with a Zeiss LSM 510/ Axiovert 100 M confocal microscope using a 63 × 1.4 NA oil immersion lens. Optical slices were scanned and recorded for three fluorophores with the pinhole sizes chosen to keep the slices 0.7 μm thick for all the three channels. Two subsequent optical slices, which had 50% overlap, were orthogonally projected and used as a 2D image. Output signals from 2 subsequent scan lines were averaged. A multi-track and multi-channel scanning procedure was used. Channel settings were for Alexa488, Argon laser (488 nm, Lasos LGK 7812 ML-1/LGN 7812, 25 mW), emission filter LP505; for Cy3, HeNe laser 1 (543 nm, Lasos LGK 7786 P, 1 mW), emission filter LP560; for Cy5, HeNe laser 2 (633 nm Lasos LGK 7628–1, 5 mW), emission filter LP650. For each track, channel separation was tested by systematic cross-excitation and detection between the channels.

6. Electrophysiology

6.1 Slice preparation and whole-cell patch-clamp recording. Adult male and female mice, aged between postnatal days 68 and 169 (P68-169), were anaesthetised with isoflurane and decapitated. The brains were removed and dissected in cold (0.5-4°C) oxygenated 'slicing' solution, containing (in mM): 85 NaCl, 2.5 KCl, 0.5 $CaCl_2$, 4 $MgCl_2$, 25 $NaHCO_3$, 1.25 NaH_2PO_4, 75 sucrose, 25 glucose, 0.01 D-(-)2-amino-5-phosphonopentanoic acid (D-AP5); pH 7.4, when bubbled with 95% O_2 and 5% CO_2. Parasagittal slices (200-250 μm) were cut from the cerebellar vermis by means of a vibrating blade microtome (HM 650V; Microm International GmbH, Walldorf, Germany). Slices were incubated at 32° C for 40 minutes and thereafter at room temperature, during which time the sucrose containing slicing solution was gradually replaced by a normal 'external' solution containing (in mM): 125 NaCl, 2.5 KCl, 2 $CaCl_2$, 1 $MgCl_2$, 25 $NaHCO_3$, 1.25 NaH_2PO_4, and 25 glucose; pH 7.4, when bubbled with 95% O_2 and 5% CO_2.

Individual slices were transferred to a submerged recording chamber and perfused with oxygenated external solution (1.5-2.5 ml/min). Neurons were directly visualized under infrared differential interference contrast optics (Zeiss Axioscop; Zeiss, Oberkochen, Germany or Olympus BX51 WI; Olympus, London, UK). All recordings were made at near physiological temperature (34-38°C), except those from *PC-$\Delta\gamma2$* mice and their littermates, which were made at room temperature (22-25° C). Whole-cell patch-clamp recordings were made with Axopatch-200A or 200B amplifiers (Molecular Devices Corporation, Sunnyvale, CA). For recordings from Purkinje cells, patch electrodes were pulled from thin-walled borosilicate glass tubing (1.5 mm o.d., 1.17 mm i.d.; G150TF-3; Warner Instruments Inc., Hamden, CT, USA), coated with Sylgard resin (Dow Corning 184), and fire polished to give a final pipette resistance of 2-4 MΩ. For molecular layer interneurons, electrodes were pulled from thick-walled glass (1.5 mm o.d., 0.86 mm i.d; GC-150F; Harvard Apparatus Ltd, Edenbridge, UK), coated with Sylgard, and fire-polished to 8-10 MΩ. Series resistance compensation (>60%; 6-9 μs lag) was used in all recordings. The 'internal' (pipette) solution contained (in mM): 140 CsCl, 4 NaCl, 0.5 $CaCl_2$, 10 N-2-hydroxyethylpiperazine-N'-2-ethanesulphonic acid (HEPES), 5 ethyleneglycol-bis (β-aminoethylether)-N,N,N',N'-tetraacetic acid (EGTA), 2 Mg-ATP; pH 7.3 with CsOH. In a few Purkinje cell recordings, tetraethylammonium (TEA) chloride (10 mM), N-(2,6-dimethylphenylcarbamoylmethyl)triethylammonium bromide (QX314; 1 mM) and (±)-methoxyverapamil hydrochloride (D600; 0.5 mM) were added to the pipette solution to block voltage-gated potassium, sodium and calcium channels. No differences were noted, and data were pooled. No correction was made for liquid junction potential.

Miniature IPSCs (mIPSCs) were recorded at –70 mV in the presence of 5 μM 6 cyano-7-nitroquinoxaline-2,3-dione disodium (CNQX), 10 μM D-AP5 and 0.5-1 μM tetrodotoxin (TTX). In all cases tested, mIPSCs recorded under such conditions were completely blocked by 10-20 μM of the $GABA_A$ receptor antagonist SR 95531 (gabazine).

6.2 Data analysis. Signals were recorded onto digital audiotape (DTR-1204; BioLogic, Claix, France; DC to 20 kHz); for analysis, replayed signals were filtered at 2 kHz (3dB, 8-pole lowpass Bessel) and digitised at 10 kHz (Digidata 1200; Axotape, Molecular Devices). Synaptic currents were detected using scaled template detection, implemented in IGOR Pro 5.0 (Wavemetrics, Lake Oswego, OR) with NeuroMatic 1.91 (http://www.neuromatic.thinkrandom.com). The detection criterion was set to include a large fraction of false positives. All detected events were subsequently assessed by eye and a minimum amplitude threshold was set at 3× the SD of an event-free epoch. In recordings from *PC-Δγ2* mice, no mIPSCs were detected, even when the detection criterion was made progressively less stringent.

Measurements of mIPSC properties were made from averaged waveforms generated from at least 70 selected events (typically 100-300), aligned on their 20% rise times. Events were included if they had a monotonic rise and if their decay was not contaminated by subsequent events. The decay of averaged mIPSCs was best described by the sum of two exponential functions according to:

$$y = A_1 \exp\left(\frac{-(x - x_0)}{\tau_1}\right) + A_2 \exp\left(\frac{-(x - x_0)}{\tau_2}\right)$$

where x_0 is the decay onset, τ_1 and τ_2 are the decay time constants of the fast and slow components, and A_1 and A_2 are their respective amplitudes. The weighted time constant of decay (τ_w) was calculated according to:

$$\tau_w = \tau_1\left(\frac{A_1}{A_1 + A_2}\right) + \tau_2\left(\frac{A_2}{A_1 + A_2}\right)$$

All drugs for electrophysiological experiments were obtained from Tocris Bioscience (Bristol, UK), except D600 which was from Sigma (Poole, UK). Zolpidem was initially dissolved in dimethyl sulfoxide (DMSO) at a concentration of 50 mM and used at 1 μM (final DMSO concentration 0.002%). Zolpidem was applied to each slice only once, and its effect on mIPSCs determined only after equilibration for at least 2 minutes.

7. Mouse behavioural experiments

The animals were housed (1-5 per cage) in transparent polypropylene macrolon cages with standard rodent pellets (Harlan Teklad Global Diet, Bicester, UK) and tap water *ad lib*. Lights were on from 7 a.m. to 7 p.m.

7.1 Basic behavioural characterization. Basic physiological and behavioural characterization of mouse phenotypes was performed according to a modified version of the primary observational screen described in the SHIRPA protocol[6,7]. The person who observed and recorded the behaviour was blind to the genotype of the animals. Particular emphasis was placed on motor characteristics: gait, spontaneous locomotor activity, horizontal wire test and righting reflex. No significant differences between the mouse lines *γ2I77lox*, *PC-Δγ2*, and *PC-γ2*–swap were observed for: body position, spontaneous activity, respiration, tremor, defecation, urination, transfer arousal, locomotor activity, palpebral closure, piloerection, gait, pelvic elevation, tail elevation, startle reflex, touch escape, positional passivity, trunk curl, limb grasping, visual placing, grip strength, pinna reflex, cornea reflex, toe pinch reflex, wire manoeuvre, provoked biting, righting reflex, contact righting reflex, negative geotaxis, body temperature, fear, irritability, aggression or vocalization. This indicates that the gene modifications did not induce any abnormal phenotypes.

7.2 Motor tests. The mice were trained during 7 days (6 trials per day) to stay on a rotating rod (diameter 4 cm, Rotamex 4/8, Columbus Instruments, Ohio, USA) for 180 s, with the rotation speed being accelerated from 5 to 30 rpm. The latency to fall from the rod in each trial was recorded and a daily average of 6 trials was calculated for each animal. The mice were also trained to walk along a 100-cm-long narrow wooden beam (0.8 cm in diameter) to the home cage on 4 consecutive days, 2 trials per day. If a mouse did not move within 10 s, it was gently pushed to induce movement. If the mouse fell from the beam, it was caught to prevent it from landing on the floor, and returned onto the beam. The latency to traverse the beam, i.e., to reach the other end of the beam, was recorded.

Zolpidem tartrate (Sanofi-Synthelabo AB, Bromma, Sweden) was crushed from a tablet and suspended in physiological saline. Flumazenil (Tocris Bioscience, Bristol, UK) was suspended in 3 % Tween 80 and brought to concentration with physiological saline. All substances were injected at 10 ml/kg body weight.

References

1. Cope, D. W. *et al*. Abolition of zolpidem sensitivity in mice with a point mutation in the $GABA_A$ receptor γ2 subunit. *Neuropharmacology* **47**, 17-34 (2004).

2. Rodriguez, C. I. *et al*. High-efficiency deleter mice show that FLPe is an alternative to Cre-loxP. *Nat Genet* **25**, 139-140 (2000).

3. Kittler, J. T. *et al*. Analysis of $GABA_A$ receptor assembly in mammalian cell lines and hippocampal neurons using γ2 subunit green fluorescent protein chimeras. Mo*l Cell Neurosc*i **16**, 440-452 (2000).

4. Smeyne, R. J. *et al*. Local control of granule cell generation by cerebellar Purkinje cells. *Mol Cell Neurosci* **6**, 230-251 (1995).

5. Mellor, J. R. *et al*. Mouse cerebellar granule cell differentiation: electrical activity regulates the $GABA_A$ receptor α6 subunit gene. *J Neurosci* **18**, 2822-2833 (1998).

6. Rogers, D. C. *et al*. Use of SHIRPA and discriminant analysis to characterise marked differences in the behavioural phenotype of six inbred mouse strains. *Behav Brain Res* **105**, 207-217 (1999).

7. Vekovischeva, O. Y. *et al*. Reduced aggression in AMPA-type glutamate receptor GluR-A subunit-deficient mice. *Genes Brain Behav* **3**, 253-265 (2004).

8. Soriano, P. Generalized lacZ expression with the ROSA26 Cre reporter strain. *Nat Genetics* **21**, 70-71 (1999)

9. Barski, J.J., Dethleffsen, K. & Meyer, M. Cre recombinase expression in cerebellar Purkinje cells. *Genesis* **28**, 93-8 (2000).

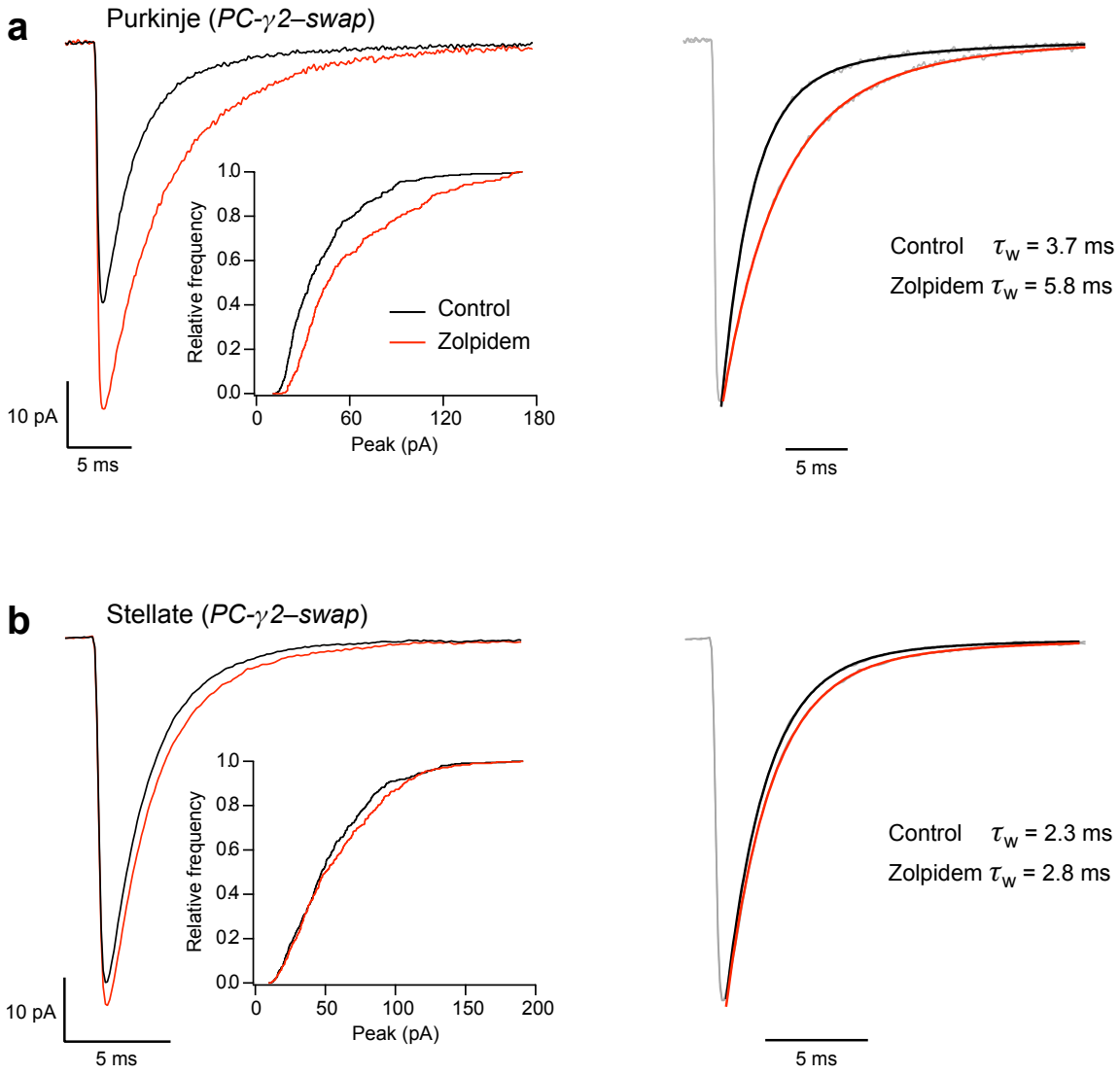

Figure S4 In slices from *PC-γ2–swap* mice, potentiation of $GABA_A$ receptor-mediated mIPSCs by zolpidem is restricted to Purkinje cells. (**a**) Representative average mIPSCs recorded at –70mV from a Purkinje cell of a P146 *PC-γ2–swap* mouse in control conditions and in the presence of zolpidem (1 μM; red, superimposed). (Note, different cell/animal to equivalent recordings shown in Fig. 4b of manuscript.) The corresponding traces on the right are shown after peak scaling. Smooth red or black lines on the decaying phase of the scaled traces (grey) are fits of double-exponential functions. Zolpidem increased the amplitude and decay of the mIPSCs. Inset shows a cumulative histogram for the amplitudes of individual mIPSCs in this cell, before, and after, zolpidem

Legend continues on following page.

(p = 1.981e-7, Kolmogorov-Smirnov test; *n* = 345, and 245 events in control and zolpidem, respectively). As seen in the scaled traces, the decay τ_w increased by ~50%. For pooled data, see Fig. 4c. (**b**) Representative averaged mIPSCs from a stellate cell in a different slice from the same PC-γ2-swap animal (details as in a). Zolpidem had no effect on the peak amplitude (inset; p = 0.271, Kolmogorov-Smirnov test; *n* = 356 and 315) and produced only a small change in the decay of the average mIPSC. Overall, in five stellate cells, zolpidem had no significant effect on amplitude (+5.2 ± 4.3%; 61.3 ± 10.4 *vs*. 63.7 ± 10.0 pA, p> 0.05) decay (τ_w; +3.0 ± 6.0%; 2.6 ± 0.1 *vs*. 2.7 ± 0.1 ms, p> 0.05) or charge transfer (+7.0 ± 5.0%; 194.4 ± 33.3 *vs*. 204.6 ± 32.3 fC, p> 0.05).